HEAT AND MASS TRANSFER IN FLOW OVER BODIES OF VARIOUS SHAPES, ALLOWING FOR BLOWING

V. I. Zinchenko and E. N. Putyatina

UDC 533.526+536.24

The authors present results of a comparative investigation of heat transfer in flow over bodies of various shapes.

The influence of blowing on the heat flux to a surface can be investigated by examining the flow over porous bodies. Here it is of interest to investigate the characteristics of the effectiveness of blowing for bodies of various shapes. Where one must account for the inertia of heat transfer in the material of the body it is expedient to consider a coupled formulation of the heat and mass transfer, since if one arbitrarily assigns the blowing distribution according to the body contour, the heat-transfer coefficient will be the unknown function and it will be difficult to use separate formulations.

We consider supersonic flow of a perfect gas over axisymmetric bodies of revolution of various shapes for a range of stagnation pressure such that different flow regimes are set up in the boundary layer. In accordance with [1-3], which deal with coupled heat transfer in the boundary layer, the formulation of the problem includes a system of nonsimilar boundary-layer equations and the unsteady heat conduction equation for a porous or a perforated material with appropriate boundary and initial conditions.

Since the boundary layer thickness for the bodies considered is much less than the minimum radius of curvature of the body, the system of equations describing the variation of average quantities in the boundary layer, using Dorodnitsyn–Lees variables, may be written as follows [3]:

$$\frac{\partial}{\partial\eta}\left(l\frac{\partial^2 f}{\partial\eta}\right)+f\frac{\partial^2 f}{\partial\eta^2}+\beta\left\{\frac{\theta}{\theta_e}-\left(\frac{\partial f}{\partial\eta}\right)^2\right\}=\alpha\left(\frac{\partial f}{\partial\eta}\frac{\partial^2 f}{\partial\eta\partial s}-\frac{\partial f}{\partial s}\frac{\partial^2 f}{\partial\eta^2}\right), \tag{1}$$

$$\frac{\partial}{\partial\eta}\left(\frac{l}{\mathrm{Pr}}\frac{\partial\theta}{\partial\eta}\right)+f\frac{\partial\theta}{\partial\eta}=\beta\gamma\frac{\theta}{\theta_e}\frac{\partial f}{\partial\eta}-l\gamma\left(\frac{\partial^2 f}{\partial\eta^2}\right)^2+\alpha\left(\frac{\partial f}{\partial\eta}\frac{\partial\theta}{\partial s}-\frac{\partial f}{\partial s}\frac{\partial\theta}{\partial\eta}\right). \tag{2}$$

Assuming that the process is one-dimensional in a porous solid and that the medium is at one temperature, one can write the energy conservation equation in the form

$$\pi_\rho\frac{\partial\theta_1}{\partial\tau}=\frac{\partial}{\partial y_1}\left(\pi_1\frac{\partial\theta_1}{\partial y_1}\right)+\frac{\partial\theta_1}{\partial y_1}\left\{\frac{r_w(\overline{\rho v})_w\sqrt{\mathrm{Re}}\,\mathrm{Pr_m}\frac{\lambda_{e0}}{\lambda_{1*}}}{r\left(1-\frac{y_1}{R_1}\right)}-\pi_1\left(\frac{\cos\psi}{r}R_N+\frac{1}{R_1-y_1}\right)\right\}. \tag{3}$$

The boundary and initial conditions can be written in the form

$$\frac{\partial f}{\partial\eta}(\infty,\ s)=1,\ \theta(\infty,\ s)=\theta_e, \tag{4}$$

$$\frac{\partial f}{\partial\eta}(0,\ s)=0,\ f(0,\ s)=f_w=-\int_0^s(\overline{\rho v})_w\left(\frac{r_w}{R_N}\right)ds\Bigg/\left[2\int_0^s\frac{\rho_e}{\rho_{e0}}\frac{\mu_e}{\mu_{e0}}\frac{u_e}{v_\mathrm{m}}\left(\frac{r_w}{R_N}\right)^2ds\right]^{0.5}, \tag{5}$$

$$q_w(0,\ s)\sqrt{\mathrm{Re}}\,\mathrm{Pr_m}\frac{\lambda_{e0}}{\lambda_{1*}}-\pi_1\theta_w^4=-\pi_1(\theta_w)\frac{\partial\theta_1}{\partial y_1}, \tag{6}$$

Scientific-Research Institute of Applied Mathematics and Mechanics, Tomsk State University. Translated from Inzhenerno-Fizicheskii Zhurnal, Vol. 45, No. 1, pp. 11-21, July, 1983. Original article submitted February 26, 1982.

0022-0841/83/4501-0717$07.50

$$\varkappa_1(\theta_{1k})\frac{\partial\theta_1}{\partial y_1}\left(\tau,\frac{L}{R_N}\right)=\sqrt{\mathrm{Re}}\,\mathrm{Pr_m}\frac{\lambda_{e\theta}}{\lambda_{1*}}(\overline{\rho v})_w\frac{r_w}{r_k\left(1-\dfrac{L/R_N}{R_1}\right)}(\theta_{-\infty}-\theta_{1k}),\tag{7}$$

$$\theta_1(0,\ y_1)=\theta_{1i}.\tag{8}$$

In writing Eqs. (1)-(8) we have used a natural system of coordinates, where s is the dimensionless length of arc, reckoned from the stagnation point along the outer profile, and η and y_1 are directed normal to the external profile of the shell in different directions. We assume that the blown gas is identical in composition with that of the incident stream and that the porosity is constant in time. Because of the assumption that the continuity equation is quasistationary for the gas phase in the porous material [4], we assume that $(\rho v)_g\varphi r\left(1-\dfrac{y_1}{R_1}\right)=r_w(\rho v)_w$ for the coordinate system used. It is also postulated that the shell thickness L, which was constant in the calculations, is considerably less than the minimum radius of curvature of the body R_1, and therefore the angle between the normals to the external and internal shell profiles is small.

To describe the turbulent flow we use a two-layer turbulent boundary layer model. In the inner region the turbulent viscosity is determined from the Prandtl formula with a Van Dreist–Sebeci damping factor [5] to account for the influence of pressure gradient and blowing:

$$\varepsilon=0{,}16\rho y^2\left\{1-\exp\left(-\frac{y}{A}\right)\right\}^2\frac{\partial u}{\partial y},$$

$$A=26\nu\sqrt{\frac{\overline{\rho}}{\tau_w}}\left\{\frac{\overline{p}}{\overline{v}_w}[1-\exp(11{,}8\overline{v}_w)]+\exp(11{,}8\overline{v}_w)\right\}^{-1/2},$$

$$\overline{p}=\frac{\nu u_e}{(\tau_w/\rho)^{3/2}}\frac{du_e}{dx},\quad \overline{v}_w=\frac{v_w}{(\tau_w/\rho)^{1/2}}.\tag{9}$$

In the outer region of the turbulent boundary layer we used the Clauser formula with a correction factor to account for transverse mixing

$$\varepsilon=0{,}0168\rho\left[1+5{,}5\left(\frac{y}{\delta}\right)^6\right]^{-1}\int_0^\infty(u_e-u)\,dy.\tag{10}$$

Here ν is the coefficient of kinematic molecular viscosity; τ_w, friction stress at the body surface; and δ, boundary-layer thickness. The boundary between the inner and outer regions was determined from the condition that the coefficients of Eqs. (9) and (10) be equal.

To calculate the flow in the transition region we used the formulas

$$l=\frac{\rho\mu}{\rho_e\mu_e}+\Gamma\frac{\rho\varepsilon}{\rho_e\mu_e},\quad \mathrm{Pr}=\frac{(\mu+\Gamma\varepsilon)\,\mathrm{Pr_m}\mathrm{Pr_t}}{\mu\,\mathrm{Pr_t}+\Gamma\varepsilon\,\mathrm{Pr_m}},\tag{11}$$

where the subscripts m and t refer to molecular and turbulent transfer; Γ is the coefficient of longitudinal mixing, which describes the flow turbulence and was suggested in [6] for the case of flow over blunt bodies:

$$\Gamma=1-\exp\left\{-\Phi r_w(s_n)\left[\int_{s_n}^{s}r_w^{-1}ds\right]\left[\int_{s_n}^{s}u_e^{-1}ds\right]\right\},$$

$$\Phi=\frac{3u_e^3}{(B\nu_e)^2}\mathrm{Re}_n^{-1,34};\quad B=60+4{,}68\mathrm{M}_n^{1,92};\tag{12}$$

Re_n, M_n are the Reynolds and Mach numbers calculated at the point of loss of stability of the laminar boundary layer. The coordinate of the stability loss point s_n, which marks the beginning of the flow transition region, was determined from the critical Reynolds number value:

$$\mathrm{Re}^{**}=\frac{u_e\rho_e\delta^{**}}{\mu_e}=200,\quad \delta^{**}=\int_0^\infty\frac{\rho}{\rho_e}\frac{u}{u_e}\left(1-\frac{u}{u_e}\right)dy.\tag{13}$$

In the laminar flow region $\Gamma = 0$, and in the turbulent region $\Gamma = 1$.

The calculations performed and a comparison with experimental data have shown that one can use this model of turbulent flow in the boundary layer with blowing present [7].

We considered flow over spherical bodies and also bodies with generator equations $y_c = x_c^{\alpha}$, $\alpha = 0.5$, $\alpha = 0.25$, $\alpha = 0.125$, $(x_c-1)^{10} + y_c^{10} = 1$ (here the dimensionless quantities x_c, y_c correspond to a Cartesian coordinate system with origin at the stagnation point and the x_c axis directed along the body axis of symmetry). For the pressure distribution over the profile of bodies of different shape we used the data of [8, 9] for supersonic flow of a perfect gas, as approximated with the help of splines.

In the numerical integration we took $Pr_m = 0.72$, $Pr_t = 1$, and the molecular viscosity was determined according to the Sutherland law. Besides the assumption that c_p is constant, the class of materials with a given porosity was restricted in such a way that the second terms can be neglected in the expressions

$$\pi_1 = \frac{\lambda_1}{\lambda_{1*}}(1-\varphi) + \frac{\lambda_g}{\lambda_{1*}}\varphi, \quad \pi_\rho = \frac{\rho_1 c_1}{\rho_{1*}c_{1*}}(1-\varphi) + \frac{\rho_g c_{pg}}{\rho_{1*}c_{1*}}\varphi$$

In solving the coupled problem it was assumed that the thermophysical characteristics of the material are constant.

The numerical integration of the boundary problem of Eqs. (1)-(8) was performed using a difference scheme obtained by means of the method of [10]. The error in approximating the original system of equations and the boundary conditions was $O(\Delta\eta)^2+O(\Delta s)$, $O(\Delta y_1)^2+O(\Delta\tau)$.

The method of calculation was analogous to that of [3]. It should be noted that in the developed turbulent flow region, one should use a larger number of nodal points in the computational region, compared with the laminar flow region, to find the asymptotic behavior of the unknown functions at the outer edge of the boundary layer. Most of the calculations were performed with a constant integration step $\Delta\eta$ across the boundary layer, although a variable step size was used in some calculations in the transverse direction, and the mesh was compressed in the viscous sublayer region. The integration step Δy_1 was varied as a function of the coupling parameter $K = \sqrt{Re Pr_m \lambda_{e0}/\lambda_{1*}}$, and for large values of K it was chosen as a variable.

In performing the numerical calculations, besides the body geometry, we also varied the governing parameters of the problem, such as the Mach number M_∞ in the incident stream, the coupling parameter K, the temperature θ_{1i}, which was chosen equal to $\theta_{-\infty}$, the stagnation point pressure p_{e0}, and the mass flow rate at the body surface $(\overline{\rho v})_w(s)$.

We now consider the results of solving the boundary problem for the case of an isothermal surface. Figure 1 shows the dimensionless heat flux q_w as a function of the longitudinal coordinate s in the boundary layer under laminar conditions.

It can be seen from Fig. 1 that for the blunter bodies (curves 2, 3, 4) the heat flux maximum is shifted to the lateral surface, toward the region where there is a minimum radius of curvature and a maximum velocity gradient at the outer edge. We note that for the shapes examined the heat flux on the lateral surface decreased with decrease of the minimum body radius of curvature. In addition, comparing Figs. 1a and b, one can see that for the laminar flow in the boundary layer the decrease of heat flux due to the influence of blowing with a given mass law $(\overline{\rho v})_w(s)$ is greater for the blunt bodies (e.g., for $(\overline{\rho v})_w = 1$ the maximum heat flux for $y_c = x_c^{0.125}$ falls by a factor of 5.6, and for $y_c = x_c^{0.5}$ it falls by a factor of 2.5, compared with the case $(\overline{\rho v})_w = 0$). This is due to the fact that for the same $(\overline{\rho v})_w$ the dimensionless flow rate $f_w(s)$ increases in absolute value for bodies with large radii of curvature in the vicinity of the stagnation point. It should be noted that for $(\overline{\rho v})_w = 0$ the distributions of heat flux obtained using [11]

$$\frac{q_w}{q_{w0}} = \frac{r\rho_w\mu_w u_e}{\sqrt{2\bar{\xi}}}\left[2\rho_{w0}\mu_{w0}\left(\frac{du_e}{dx}\right)_0\right]^{-1/2}\frac{\theta_{\eta w}}{\theta_{\eta w0}},$$

$$\bar{\xi} = \int_0^x \rho_w\mu_w u_e r_w^2\,dx, \quad \frac{\theta_{\eta w}/(1-\theta_w)}{\theta_{\eta w0}/(1-\theta_{w0})} = \frac{1+0.096\sqrt{\bar{\beta}}}{1.068}, \quad \bar{\beta} = \frac{2\bar{\xi}}{u_e}\cdot\frac{du_e}{d\bar{\xi}}$$

for the different body shapes in the constant surface temperature case coincide to an accuracy of 1-2% with the corresponding distributions of q_w obtained from calculations in the Mach number range examined.

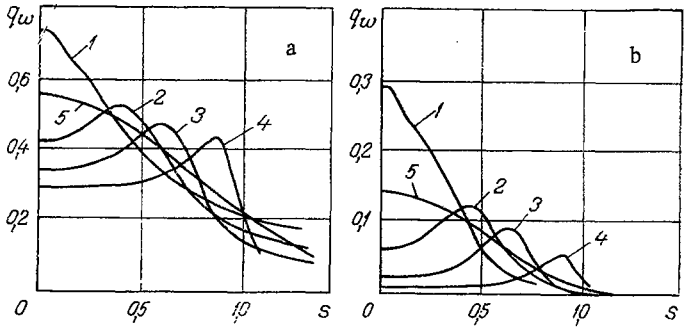

Fig. 1. The dimensionless heat flux as a function of the longitudinal coordinate s: 1, 2, 3) flow over bodies with profile equations $y_c = x_c^{\alpha}$, $\alpha = 0.5$, 0.25, and 0.125, respectively; 4) $(x_c-1)^{10} + y_c^{10} = 1$; 5) a sphere, $(x_c-1)^2 + y^2 = 1$, $M_\infty = 4$, $T_\infty = 288°K$, $T_w = 300°K$; a) $(\overline{\rho v})_w = 0$; b) $(\overline{\rho v})_w(s) = \text{const} = 1$.

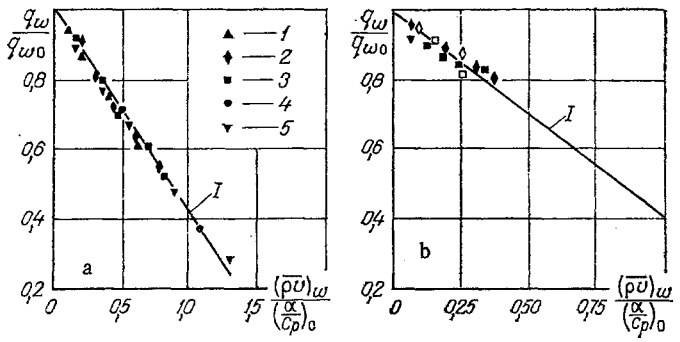

Fig. 2. The ratio q_w/q_{w0} as a function of the relative flow rate $(\overline{\rho v})_w/\left(\frac{\alpha}{c_p}\right)_0$: 1, 2, 3) $y = x^{\alpha}$, $\alpha = 0.5$, 0.25, and 0.125, respectively; 4) a sphere; 5) $x^{10} + y^{10} = 1$.

Figure 2a shows the ratio q_w/q_{w0} as a function of the relative flow rate $(\overline{\rho v})_w/\left(\frac{\alpha}{c_p}\right)_0$, where $\left(\frac{\alpha}{c_p}\right)_0 = \frac{q_{w0}}{1-\theta_{w0}}$ and q_{w0} are found with no blowing. Line I was obtained using the relation of [12], constructed for the vicinity of the stagnation point:

$$q_w/q_{w0} = 1 - k(\overline{\rho v})_w/\left(\frac{\alpha}{c_p}\right)_0, \quad k = 0.57 - 0.61. \tag{14}$$

The points denote the ratios q_w/q_{w0} obtained for the bodies considered in the region of the maximum heat flux under laminar flow conditions. The values of the original parameters coincide with the corresponding values for Fig. 1.

It can be seen from Fig. 2 that for moderate blowing levels Eq. (14) can be used for bodies where the maximum heat flux $q_w(s)$ is obtained on the lateral surface in a region beginning at the stagnation point, up to values of s corresponding to the maximum heat flux.

In [13] the efficiency of porous cooling for a sphere was derived as the ratio of the total heat flux when screened due to blowing to the total mass flow rate of the blown gas:

$$H_L = \frac{\int_0^{s_k} r_w q_{w0} ds - \int_0^{s_k} r_w q_w ds}{(H_e - H_w)\int_0^{s_k} r_w (\rho v)_w ds}, \tag{15}$$

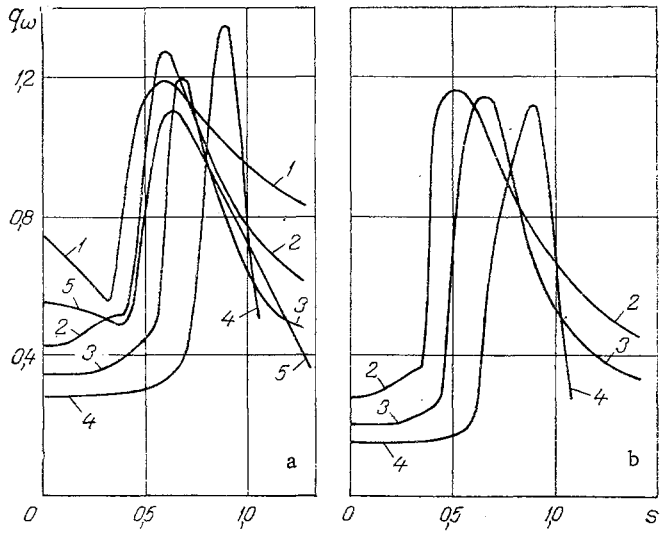

Fig. 3. The dimensionless heat flux q_w as a function of the longitudinal coordinate s: curves 1, 2, and 3 were constructed for bodies with generator equations $y_c = x_c^{\alpha}$, $\alpha = 0.5$, 0.25, and 0.125, respectively; 4) $(x_c-1)^{10} + y_c^{10}$; 5) a sphere, $M_\infty = 4$, $T_\infty = 288°K$, $T_w = 300°K$, $p_{e0} = 5.56 \cdot 10^5$ N/m^2, $R_N = 0.1$ m; a) $(\overline{\rho v})_w = 0$; b) $(\overline{\rho v})_w = 0.3$.

and hence it follows that the larger H_L, the higher the efficiency. In our case, in considering bodies of different shape we shall compare the total heat flux in the presence and absence of blowing $\int_0^s r_w q_w ds$ and $\int_0^s r_w q_{w0} ds$ under conditions of either the same areas over which the blowing is distributed or the same values of $y_c = 1$ and the same total flow rate $\int_0^s r_w (\rho v)_w dx$ for the different bodies. This comparison shows that with the mass flow rate laws $(\overline{\rho v})_w(s) = \text{const}$ the total heat flux for the blunter bodies is less than for a sphere and a body with the profile equation $y_c = x_c^{0.5}$ in both the first and the second cases (e.g., for the same areas $\Pi = 4.27$, $\int_0^s r_w q_{w0} ds = 0.226$ for $y_c = x_c^{0.5}$, $\int_0^s r_w q_{w0} ds = 0.182$ for $y_c = x_c^{0.125}$, and for $(\overline{\rho v})_w = 1$ the values of $\int_0^s r_w q_w ds$ are 0.0234 and 0.0181, respectively).

Thus, analysis of the local and the integrated heat-transfer characteristics shows that for laminar flow conditions in the boundary layer one can reduce the heat flux to the body by using blunt bodies.

We now consider flow for values of the Reynolds number that give laminar, transitional and turbulent flow conditions in the boundary layer.

Figure 3 shows the behavior of the dimensionless heat flux $q_w(s)$ with laminar, transitional, and turbulent flow regions in the boundary layer and with constant surface temperature. The calculations were performed for $(\overline{\rho v})_w = 0$ (Fig. 3a) and $(\overline{\rho v})_w = 0.3$ (Fig. 3b). Curves 1-5 correspond to the same body shapes as in Fig. 1. It can be seen from Fig. 3a that on the lateral part of the surface, where laminar flow conditions obtain in the boundary layer, the values of $q_w(s)$ coincide with the curves of Fig. 1a. In the transition region and in the developed flow turbulence region the heat flux increases markedly compared with the corresponding curves for laminar flow in the boundary layer. Here, as can be seen from Fig. 3a, for the blunter bodies (curves 3, 4) the zone where the maximum heat flux is found is shifted slightly back along the body profile compared with the position of the maximum $q_w(s)$ for laminar flow conditions.

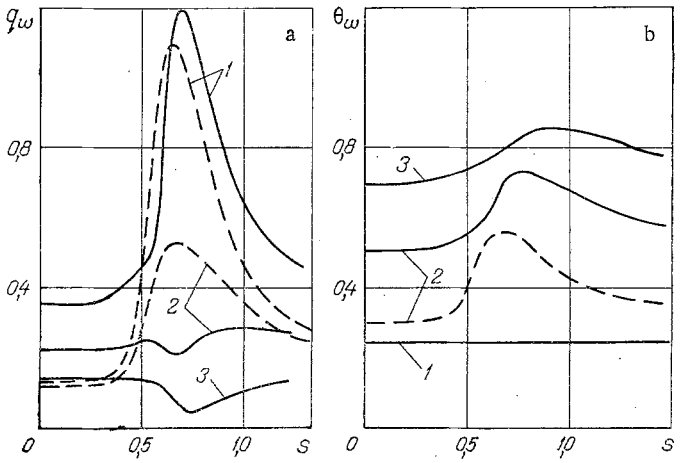

Fig. 4. The dimensionless heat flux q_W (a) and the reduced surface temperature θ_W (b) as a function of the longitudinal coordinate s at various times. The calculations have been made for the body with the profile equation $y_c = x_c^{0.125}$, $M_\infty = 4$, $T_\infty = 288°K$, $T_{ii} = 300°K$, $p_{e0} = 5.56 \cdot 10^5$ N/m^2, $R_N = 0.1$ m; the solid lines correspond to an impermeable wall, and the broken lines were obtained for $(\overline{\rho v})_W = 0.5$, K = 3.187; 1) $\tau = 0$; 2) 0.03; 3) 0.07.

It should be noted that the calculated results agree satisfactorily, in regard to location and value of the maximum heat flux and for the body shapes examined, with the formula for $q_W(s)$ of [14], obtained for developed turbulent flow. It can be seen from the figures that in developed turbulent flow the maximum heat flux values are close for the different bodies. Calculations have shown for large stagnation pressure values that the location and value of the maximum heat flux is independent of whether or not the transition flow region is taken into account.

As one might expect, with blowing of gas into the boundary layer there is destabilization of the flow and the point of loss of stability for the different bodies is shifted toward the stagnation point (curves 2, 3, 4 of Fig. 3b). Therefore, for some values of s the heat flux with blowing becomes larger than the corresponding q_W with no blowing, because of the flow becoming turbulent earlier.

Figure 2b shows the ratio q_W/q_{W0} as a function of $(\overline{\rho v})_w / \left(\frac{\alpha}{c_p}\right)_0$, obtained for the region of developed flow turbulence. Curve 1 was obtained using Eq. (14); the open points correspond to s = 0.6, and the solid points to s = 0.8. It can be seen from Fig. 2b that for moderate blowing levels ($(\overline{\rho v})_W \leqslant 0.5$) the ratio q_W/q_{W0} obtained from Eq. (14) is close to the calculated value, so that one can use Eq. (14) for the bodies $y_c = x_c^{0.25}$, $y_c = x_c^{0.125}$, $(x_c - 1)^{10} + y_c^{10} = 1$ at moderate blowing in the developed turbulent flow region.

A comparison of total heat flux for the case with laminar, transitional, and turbulent flow regions in the boundary layer has shown that for bodies with a smaller radius of curvature, the values of total heat flux reaching the body per unit time also become less (e.g., when we consider the same surface area $\Pi = 4.27$, for $(\overline{\rho v})_w = 0$ $\int_0^s r_w q_{w0} ds = 0.49$ for the body with the equation $y_c = x_c^{0.125}$, $\int_0^s r_w q_{w0} ds = 0.65$ for the case $y_c = x_c^{0.5}$, and for $(\overline{\rho v})_W = 0.5$ these values are equal to 0.39 and 0.55, respectively).

From this viewpoint it is also expedient to use a body of blunted shape, but one must remember that in this case the maximum local heat flux remains practically the same for all the bodies.

We now consider the results of solving the coupled problem. Figure 4 shows the dimensionless heat flux $q_w(s)$ (a) and the surface temperature $\theta_w(s)$ (b) at various times for the case where various flow regimes are found in the boundary layer. Here the calculations were made for the case $y_c = x_c^{0.125}$. The solid curves were drawn for flow without blowing, and the broken lines for flow with $(\overline{\rho v})_w = 0.5$. It follows from the solution of the coupled heat transfer problem that for flows with large Reynolds number the surface temperature in the maximum flux region takes on a high value as time goes on, which leads to a subsequent decrease of heat flux and to the occurrence of minimum value of $q_w(s)$ for these sections of the lateral surface. However, for the spherical body, as time goes on, the qualitative behavior of $q_w(s)$ does not change in comparison with the distribution of $q_w(s)$ at $\tau = 0$. This is associated with a difference in the behavior of $T_e(s)$ for bodies of this shape.

From the results of solving the boundary problem of Eqs. (1)-(8) for the case of low stagnation pressures (laminar flow) we also see that for bodies with a nonmonotonic heat flux behavior along the body profile, the surface temperature distribution $\theta_w(s)$ is nonmonotonic as time goes on (the equations of the profiles are $y_c = x_c^{0.25}$, $y_c = x_c^{0.125}$, $(x_c-1)^{10} + y_c^{10} = 1$). Here the ratio of Stanton numbers $\frac{St}{St_0}(s, \tau) = \frac{q_w/(1-\theta_w)}{q_{w0}/(1-\theta_{w0})}$, where St_0 is the value at the stagnation point, is not a conservative function of the process, as was shown for a sphere in [2], and as occurs for the body with $y_c = x_c^{0.5}$, where the value of St/St_0 varies by at most 15-18% for large values of s.

For the same governing parameters we examined the problem of heating of a body (with profile equation $y_c = x_c^{0.125}$), where we use the relation obtained in [11] as a boundary condition for the gas phase. The difference in regard to surface temperature with the results of solving the coupled problem was 40% in the maximum flux region at the same values of time.

Thus, in the laminar flow regime in the boundary layer, for bodies of blunt shape with a nonmonotonic behavior of $q_w(s)$ and $\theta_w(s)$, the ratio of the numbers St/St_0 varies considerably with time, and the use of a heat-transfer coefficient found for the isothermal-wall case leads to appreciable errors in determining important practical quantities. The same situation arises for bodies of the above geometry at large values of p_{e0} for complex flow regimes in the boundary layer, which also leads to a need to solve the coupled problem.

NOTATION

ξ, $\eta = \frac{u_e r}{\sqrt{2\xi}} \int_0^y \rho dy$, Dorodnitsyn–Lees variables; s, dimensionless arc length, reckoned from the forward stagnation point; x, y, axes in a body-fixed coordinate system; f, dimensionless stream function; $f'_\eta = u/u_e$, dimensionless velocity; $\alpha = \left(2\int_0^s \rho_e\mu_e u_e (r_w/R_N)^2 ds\right) \Big/ (\rho_e\mu_e u_e (r_w/R_N)^2)$,

$\beta = \alpha_i/u_e \cdot du_e/ds$, $\gamma = u_e^2/c_p T_{e0}$, dimensionless parameters; $q_w = \lambda_w \frac{\partial T}{\partial y}\Big|_w \frac{\sqrt{\mathrm{Re}}}{v_m \rho_{e0} h_{e0}}$, dimensionless heat flux; Pr, $\mathrm{Re} = v_m \rho_{e0} R_N/\mu_{e0}$, $v_m = \sqrt{2H_{e0}}$, Prandtl and Reynolds numbers, and maximum velocity; $\theta = T/T_{e0}$, dimensionless temperature; H, ρ, c_p, enthalpy, density, and specific heat, respectively; μ, λ, coefficients of viscosity and thermal conductivity; $(\rho v)_w$, flow rate of gas through the porous shell; $(\overline{\rho v})_w = (\rho v)_w \frac{\sqrt{\mathrm{Re}}}{v_m \rho_{e0}}$, dimensionless flow rate of gas through the porous shell; R_1, dimensionless radius of curvature of the wetted profile at a given point; ψ, angle between the tangent to the contour and the x_c axis; $y_1 = -y/R_N$, $\tau = t/t^*$, dimensionless coordinate in the solid body and dimensionless time; t, physical time; $t^* = R_N \rho_{1*} c_{1*}/\lambda_{1*}$, characteristic time; R_N, characteristic body dimension; L, thickness of porous shell; σ, Stefan–Boltzmann constant; ε, emissivity; φ, porosity; $St = q_w v_m h_{e0} \rho_{e0}/\sqrt{\mathrm{Re}}\,\rho_\infty v_\infty c_p (T_{e0} - T_w)$ Stanton number. Subscripts: e, e0, w, k, values at the outer edge of the boundary layer, at the outer edge at the stagnation point, on the body surface, and at the inner wall of the shell at $y_1 = L/R_N$; 1, characteristic of the solid component of the porous shell, temperature of the porous material; g, gaseous component in the porous body; li, temperature at the initial time; ∞, gas temperature in the shell cavity; *, characteristic values.

LITERATURE CITED

1. A. V. Lykov, Heat and Mass Transfer (Handbook) [in Russian], Énergiya, Moscow.

2. V. I. Zinchenko and E. G. Trofimchuk, "Solution of nonsimilarity problems in laminar boundary-layer theory, allowing for coupled heat transfer," Izv. Akad. Nauk SSSR, Mekh. Zhidk. Gaza, No. 4, 59 (1977).
3. V. I. Zinchenko and E. G. Trofimchuk, "Solution of nonsimilarity problems in boundary-layer theory, allowing for unsteady coupled heat transfer and blowing," Inzh.-Fiz. Zh., 38, No. 3, 543 (1980).
4. B. M. Pankratov, Yu. V. Polezhaev, and A. K. Rud'ko, Interaction of Materials with Gas Flux [in Russian], Mashinostroenie, Moscow (1976).
5. T. Sebeci, "Turbulent flow over a porous wall in the presence of a pressure gradient," Raketn. Tekh. Kosmonavt., 8, No. 12, 48 (1970).
6. K. Chen and N. Tyson, "The application of the Emmons turbulent spot theory to flow over blunt bodies," Raketn. Tekh. Kosmonavt., No. 5, 63 (1971).
7. V. I. Zinchenko, E. N. Putyatina, and E. G. Trofimchuk, "Calculation of the characteristics of coupled heat and mass transfer with a sharp variation in boundary conditions," Heat and Mass Transfer VI, Vol. 1, Pt. 2 [in Russian], A. V. Lykov ITMO, Minsk (1980).
8. S. M. Gilinskii and G. F. Telenin, "Supersonic flow over bodies of different shape with a detached shock wave," Izv. Akad. Nauk SSSR, Mekh. Mashinostr., No. 5, 148 (1964).
9. L. N. Lyubimov and V. V. Rusanov, Flow of a Gas Over Blunt Bodies [in Russian], Vol. 2, Nauka, Moscow (1970).
10. A. M. Grishin and V. N. Bertsun, "An iteration-interpolation method and the theory of splines," Dokl. Akad. Nauk SSSR, 214, No. 4, 751 (1974).
11. Kemp, Rose, and Detra, "Laminar heat transfer to blunt bodies in flow of dissociated air," in: Gasdynamics and Heat Transfer in the Presence of Chemical Reactions [Russian translation], IL, Moscow (1962).
12. N. A. Anfimov and V. V. Al'tov, "Heat transfer, friction, and mass transfer in the laminar multicomponent boundary layer with blowing of dissimilar gases," Teolofiz. Vys. Temp., No. 3, 409 (1965).
13. Kubota and Karashima, "Heat shielding problem with local mass injection at multiple stations," Jp. Soc. Aernaut. Space Sci., 4, No. 26, 85 (1971).
14. V. S. Avduevskii, B. M. Galitseiskii, G. A. Glebov, et al., Basic Heat Transfer in Aviation and Rocket Technology [in Russian], Mashinostroenie, Moscow (1975).

POSSIBILITY OF RAPID DETERMINATION OF TURBULENCE GENERATION IN A LAMINAR BOUNDARY LAYER

E. I. Polyak

UDC 532.526.3

An engineering method is proposed for determining the initiation of turbulence in a subsonic ($M \leqslant 1$) laminar boundary layer with a heat supply in the presence of a pressure gradient and injection.

A large number of theoretical and experimental works have by now been devoted to the question of the transition of a laminar boundary layer into a turbulent boundary layer. However, this phenomenon (transition from laminar to turbulent boundary layer) is not amenable to rational explanation in every sense. What is needed is a methodological approach which considers both theoretical and empirical aspects of the phenomenon. Possible elements of such an approach, presented below, permit consideration of some of these aspects.

To determine the moment of loss of stability of the laminar boundary layer on the body under consideration, it is necessary to have estimates of the velocity profiles of this layer along the generatrix of the body. However, such estimates are often lacking, or obtaining them proves to be a very complex task. Thus, the stability of an incompressible laminar boundary layer is often determined by using the approximate velocity profile of K. Pohlhausen [1], which adequately describes the solutions of the equation of an incompressible boundary layer in the presence of a pressure gradient:

Translated from Inzhenerno-Fizicheskii Zhurnal, Vol. 45, No. 1, pp. 21-25, July, 1983. Original article submitted March 31, 1982.

 0022-0841/83/4501-0724$07.50